

## Supplementary Information

### 1 DFT-Methods

Density functional theory (DFT) calculations were based on the full-potential linear augmented plane wave (FP-LAPW) method, as implemented in the band structure program ELK<sup>1</sup>. The local density approximation has been used to determine the exchange-correlation potential.

Due to the need to describe a significant area surrounding the defect we have used larger supercells (SC) up to  $5 \times 5 \times 1$  repetitions of the unit cell comprising 4 atoms, hence 100 atoms in the simulation. Within the periodic supercell an 8.5Å thick vacuum spacer was included to approximate the effect of the surface. The full Brillouin zone has been sampled by  $5 \times 5 \times 1$   $k$ -points.

STM images were simulated using the Tersoff-Hamann approach<sup>2</sup>, a method thoroughly validated for a huge number of materials<sup>3</sup>. The tunneling current for the applied (negative) bias  $V$  is then assumed to be proportional to the energy-resolved charge density  $n(r, E)$  integrated within the appropriate energy range:

$$I(r, V) \propto \int_{E_F - eV}^{E_F} n(r, E) dE \quad (1)$$

Here  $E_F$  denotes the Fermi energy and  $r(x, y, z)$  the position of the tip. In our calculations,  $z = 0$  defines the scanning plane above the surface atom plane, which we assume to be at  $z = 0.06$  distance. We have employed existing functions in the ELK code to obtain the charge density, but a custom modification was needed to evaluate it in an arbitrary specified energy range. In STM experiments, bias voltages between  $V = -1.2$  V and  $V = -1.4$  V showed the best contrast for our purposes. For our calculations we used energy ranges of the same order, mostly  $\Delta V = 1.3$  V. The presence of a defect in a finite size supercell leads to a shift of the Fermi level, but the calculated STM figures are to be compared to the experimental situation where all defects are seen within one sample, thus with a constant Fermi level. Therefore for the evaluation of Eq. (1) we shift the Fermi level so that the valence band top matches that of the ideal sample.

The DOS was calculated from a  $3 \times 3 \times 1$  supercell.

## 2 XPS core level fitting

XPS core level data was measured using an Omicron NanoESCA spectrometer and an Al  $K_{\alpha}$  X-ray source. Fitting of XPS core level spectra was done in the program KolXPD [[https:// www.kolibrik.net/kolxpd](https://www.kolibrik.net/kolxpd)]. The estimation of the relative concentrations between tin, sulfur, and iron are based on respective fitting of spin-orbit split Voigt doublet areas of Sn  $4d$ , S  $2p$ , and Fe  $3p$  core levels, which are normalized to calculated photoionization cross sections<sup>4</sup>. A Shirley background is assumed in all cases.

## 3 Supplementary STM data

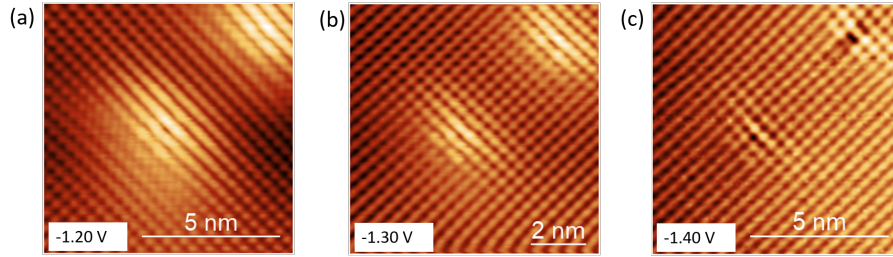


Figure 1: STM contrast obtained from the mound-like defect at (a)  $V_{\text{bias}} = -1.2 \text{ V}$  (b)  $V_{\text{bias}} = -1.3 \text{ V}$  and (c)  $V_{\text{bias}} = -1.4 \text{ V}$  [ $I_{\text{set}} = 20 \text{ pA}$ ].

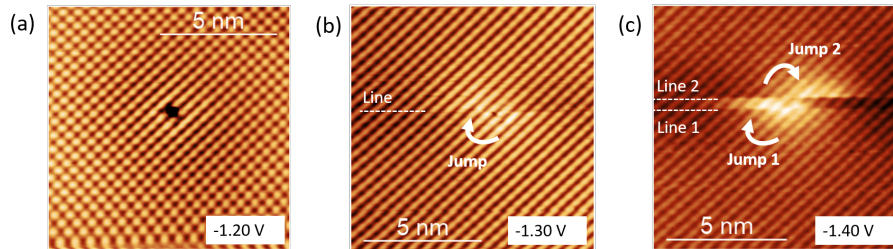


Figure 2: STM contrast obtained from the mobile defect at (a)  $V_{\text{bias}} = -1.2 \text{ V}$  (b)  $V_{\text{bias}} = -1.3 \text{ V}$  and (c)  $V_{\text{bias}} = -1.4 \text{ V}$  [ $I_{\text{set}} = 20 \text{ pA}$ ]. The defect is manipulated in the x-direction as the tip scans the surface for  $V_{\text{bias}} = -1.3$  and  $-1.4 \text{ V}$ . In the latter case two manipulation events appeared in line 1 and line 2 (dashed horizontal lines). It is important to note that before and after manipulation events, bright Sn atom rows remain at the same position, proving that the tip has not changed during these events.

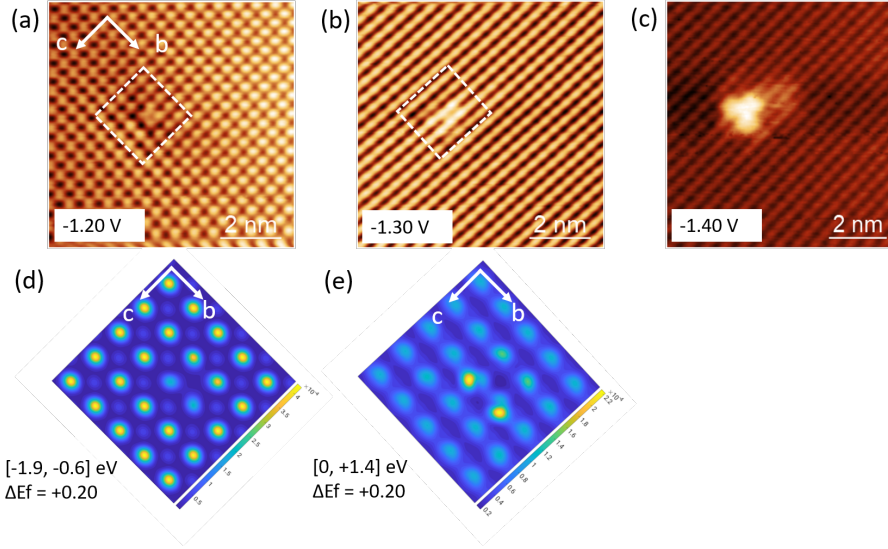


Figure 3: STM contrast obtained from  $V_S$  defect at (a)  $V_{\text{bias}} = -1.2$  V, (b)  $V_{\text{bias}} = -1.3$  V, and (c)  $V_{\text{bias}} = -1.4$  V [ $I_{\text{set}} = 20$  pA]. Dashed boxes indicate the scale of DFT calculated images below. (d) and (e) show DFT calculated images for the same defect, integrated over negative and positive energy ranges in the DOS, respectively.

## 4 Sample preparation

S and Sn of 5N purity were used for the synthesis of  $\text{Sn}_{1-x}\text{Fe}_x\text{S}$ . For iron doping, Fe ( $>4\text{N}$ ) was used in the form of  $\text{Fe}_{0.49}\text{S}_{0.51}$ , which was pre-synthesized by heating the Fe and S mixture at 1073 K for 4 weeks. All elements were provided by Merck. The synthesis was carried out by heating a stoichiometric mixture of Sn, S and  $\text{Fe}_{0.49}\text{S}_{0.51}$  in evacuated and sealed quartz vials ( $10^{-3}$  Pa) at 1223 K for 12 hours in a horizontal furnace. Subsequent crystal growth was carried out by cooling to room temperature at a rate of 6 K per hour. This free-melt crystallization (FMC) process yielded single crystals of approximately 10 mm in length, 3-6 mm in width and up to 2 mm in thickness. The in situ deposition of Fe on SnS was done using a standard Omicron e-beam evaporator. During deposition the sample was at room temperature. The calibration of the evaporator flux was done via STM on submonolayer Fe island coverages on clean Au(111) after verification of the Au(111) herringbone reconstruction.

## References

- [1] <http://elk.sourceforge.net/>.
- [2] J. Tersoff and D. R. Hamann, **31**, 805–813.

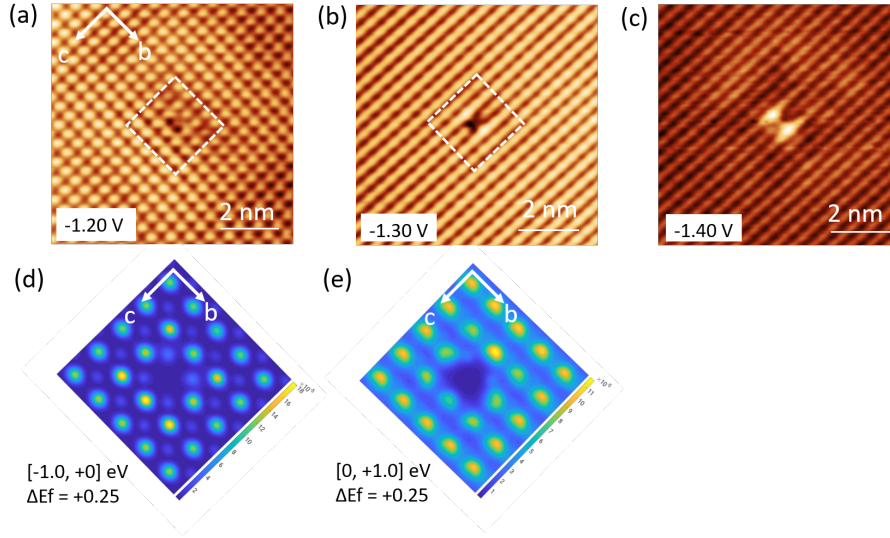


Figure 4: STM contrast obtained from coupled ( $V_{\text{Sn}}$ ,  $\text{Fe}_{\text{Sn}}$ ) defect at (a)  $V_{\text{bias}} = -1.2 \text{ V}$ , (b)  $V_{\text{bias}} = -1.3 \text{ V}$ , and (c)  $V_{\text{bias}} = -1.4 \text{ V}$  [ $I_{\text{set}} = 20 \text{ pA}$ ]. Dashed boxes indicate the scale of DFT calculated images below. (d) and (e) show DFT calculated images for the same defect, integrated over negative and positive energy ranges in the DOS, respectively.

- [3] K. Choudhary, K. F. Garrity, C. Camp, S. V. Kalinin, R. Vasudevan, M. Ziatdinov and F. Tavazza, **8**, year.
- [4] J. Yeh and I. Lindau, *Atomic Data and Nuclear Data Tables*, 1985, **32**, 1–155.